View metadata, citation and similar papers at core.ac.uk

brought to you by CORE

provided by Queensland University of Technology ePrints Archive

Queensland University of Technology
Brisbane Australia

This is the author's version of a work that was submitted/accepted for publication in the following source:

Kairn, Tanya, Crowe, Scott, & Markwell, Tim
(2015)
Use of 3D printed materials as tissue-equivalent phantoms. In
Jaffray, David A. (Ed.)
IFMBE Proceedings: World Congress on Medical Physics and Biomedical Engineering, Springer, Toronto, Canada, pp. 728-731.

This file was downloaded from: https://eprints.qut.edu.au/86643/

© Copyright 2015 Springer International Publishing Switzerland

The final publication is available at Springer via http://dx.doi.org/10.1007/978-3-319-19387-8_179

Notice: *Changes introduced as a result of publishing processes such as copy-editing and formatting may not be reflected in this document. For a definitive version of this work, please refer to the published source:*

https://doi.org/10.1007/978-3-319-19387-8_179

Use of 3D Printed Materials as Tissue-Equivalent Phantoms

T. Kairn[1,2], S. B. Crowe[2,3] and T. Markwell[4]

[1] Genesis CancerCare Queensland, Auchenflower, Australia
[2]Queensland University of Technology, Brisbane, Australia
[3]Cancer Care Services, Royal Brisbane and Women's Hospital, Herston, Australia
[4]Mater Radiation Oncology, South Brisbane, Australia

Abstract— **This study used the specific example of 3D printing with acrylonitrile butadiene styrene (ABS) as a means to investigate the potential usefulness of benchtop rapid prototyping as a technique for producing patient specific phantoms for radiotherapy dosimetry. Three small cylinders and one model of a human lung were produced via in-house 3D printing with ABS, using 90%, 50%, 30% and 10% ABS infill densities. These phantom samples were evaluated in terms of their geometric accuracy, tissue equivalence and radiation hardness, when irradiated using a range of clinical radiotherapy beams. The measured dimensions of the small cylindrical phantoms all matched their planned dimensions, within 1mm. The lung phantom was less accurately matched to the lung geometry on which it was based, due to simplifications introduced during the phantom design process. The mass densities, electron densities and linear attenuation coefficients identified using CT data, as well as the results of film measurements made using megavoltage photon and electron beams, indicated that phantoms printed with ABS, using infill densities of 30% or more, are potentially useful as lung- and tissue-equivalent phantoms for patient-specific radiotherapy dosimetry. All cylindrical 3D printed phantom samples were found to be unaffected by prolonged radiation and to accurately match their design specifications. However, care should be taken to avoid oversimplifying anatomical structures when printing more complex phantoms.**

Keywords— **Radiation therapy, rapid prototyping, lung phantom.**

I. Introduction

Three dimensional (3D) models of anatomical structures produced via rapid prototyping are being increasingly adopted for use in maxillofacial surgery planning [1], haemodynamics studies [2,3] and other medical applications [3,4]. Geometrically accurate models can be designed using medical images acquired using MRI [2,4] or CT [5,6,7] and inexpensively fabricated using polymers including polyeurethane [5], polylactic acid [8] and epoxy resins [5]. Materials and densities can be varied to produce radiographic contrast or tissue-equivalence [5,6].

Clearly, such models would be useful as radiotherapy phantoms, for patient-specific quality assurance or treatment plan evaluation in anatomically challenging or dosimetrically complex cases. To date, however, the use of rapid protoyping for the construction of radiotherapy phantoms has been largely limited to generic models based on average patient anatomy, for use in routine clinical dosimetry [9] or national and international dosimetry audits [5,6].

The broad adoption of a rapid prototyping technique for the production of patient specific phantoms for use in radiotherapy dosimetry requires that the resulting phantoms are shown to accurately replicate the desired patient geometries, be sufficiently tissue-equivalent to provide usable measurements and be insusceptible to the effects of radiation.

In this study, therefore, several samples of an acrylonitrile butadiene styrene (ABS) phantom material, produced quickly and inexpensively via 3D printing, were evaluated in terms of their geometric accuracy, tissue equivalence and radiation hardness, so that 3D printing may be more broadly adopted for phantom construction in the future.

II. Materials and Methods

A. Phantom construction

Four small samples of phantom material were evaluated in this study. Three of these were cylinders, designed using Sketchup 2014 (Trimble Navigation Ltd, Sunnyvale, USA) to fit into a CIRS 062 CT calibration phantom (Computerized Imaging Reference Systems Inc., Norfolk, USA). The remaining sample was a 50 % scale model of a human lung, based on CT data.

The CT images used to create the small lung phantom were acquired at a 2.5 mm slice thickness, using a GE DIscovery 690 scanner operating at 120 kVp. These images were imported into Deasy et al's CERR code [10], where the the lung and a small peripheral tumour were contoured. Stereolithography (STL) format files describing the contours were then produced using Fedorov et al's 3D Slicer code [11] and smoothed using the Meshmixer 3D modelling software (Autodesk Inc., Mill Valley, USA).

The STL geometry files for all of the sample phantoms were imported into the XYZware 3D printing software and printed in ABS using a Da Vinci 3D pinter (XYZ printing, San Diego, USA) which converted the STL file to machine

commands (gcode) to enable printing. Because ABS has a density of 1.05 g/cm^3, the polymer was printed in a mesh pattern, with air filling the gaps between solid strands of ABS, to produce some lower density materials. The three cylinders were printed with 30%, 50% and 90% ABS infill densities and the small lung phantom was printed with a 10% ABS infill density.

B. Geometric evaluation

The simple cylinders were measured physically, with calipers, and radiologically, by CT scanning the phantom and using the measurement tool in the Varian Eclipse radiotherapy treatment planning system (Varian Medical Systems, Palo Alto, USA) to measure the phantom's features in the imported CT data. These measurement results were compared with the design dimensions for the cylinders.

The dimensions of the small lung phantom were evaluated qualitatively, by CT scanning the phantom and comparing the resulting images with images of the lung in the original patient CT data on which the phantom was based.

C. Tissue equivalence

The tissue equivalence of the sample phantoms was assessed via two methods. Firstly, the phantoms were imaged using a Siemens AS Open CT scanner (Siemens Healthcare, Malvern, USA) and the Hounsfield units from the resulting scan were used to identify the materials' linear attenuation coefficients and to derive their mass densities and electron densities. These results were compared with corresponding data for lung- and water-equivalent inserts from a Gammex 467 tissue characterisation phantom.

The attenuation and scatter properties of the cylindircal samples were also evaluated, for a range of clinical radiotherapy beams. Eight different single-field treatments were planned for a phantom consisting of 30 x 30 x 7 cm^3 of Virtual Water (Standard Imaging, Middleton, USA) with the three cylindical samples positioned on top, along with five samples of lung-, tissue- and water-equivalent plastic from the tissue characterisation phantom.

The treatment beams used in the plans were a 10 MV flattened photon beam, a 6 MV flattened photon beam, and a 6 MV unflattened (FFF) photon beam, as well as 6, 9, 12, 16 and 20 MeV electron beams, delivered using a Varian Truebeam linear accelerator. The field size used for all beams was 25 x 25 cm^2 and the surface of the Virtual Water block was set at 105 cm from the photon source.

Each of these treatments was delivered to the phantom, with a 20 x 20 cm^2 sheet of EBT3 radiochromic film placed between the Virtual Water block and the cylindrical inserts. The film was calibrated, scanned and analysed using an established film dosimetry procedure [12,13] and the results were compared with the doses predicted by the Varian Eclipse treatment planning system.

D. Radiation hardness

The effects of radiation on the 3D printed phantoms was evaluated by re-measuring the geometry of the cylindrical samples and re-acquiring the CT scan used in the tissue equivalence study after the three samples had been irradiated for several hours a day for 30 days, while placed on the floor below a 3D water tank during the commissioning of a new linear accelerator. Results obtained before and after this substantial irradiation were compared, in order to identify any geometric or chemical changes in the samples.

III. Results and Discussion

A. Geometric evaluation

Table 1 Measured dimensions of sample phantoms

ABS infill density	Meas. method	Diameter (cm)	Length (cm)
90%	Design	3.0	4.0
90%	Physical	3.0	3.9
90%	Phantom CT	2.9	3.9
50%	Design	3.0	4.0
50%	Physical	3.0	3.9
50%	Phantom CT	3.0	3.9
30%	Design	3.0	4.0
30%	Physical	3.0	3.9
30%	Phantom CT	3.0	3.9

Table 1 shows the results of the geometric evaluation of the phantom samples and indicates that the (physically and radiologically) measured dimensions of the small cylindrical phantoms closely matched their planned dimensions.

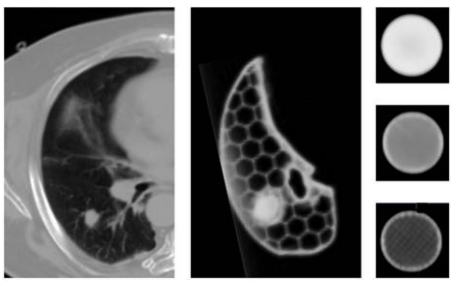

Fig. 1 CT images of patient's lung (left) and resulting lung phantom (right), alongside CT images of cylindrical samples with (from top to bottom) 90%, 50% and 30% ABS infill density.

Qualitative comparison between the CT images of the 3D-printed lung phantom and the patient CT on which it was based revealed more substantial differences. The use of manual contours to produce an initial design from the CT images led to some simplification of the shape of the lung and some conservative over-estimation of the size of the tumour. The overall shape of the lung volume was further simplified as the design was refined and prepared for printing. These effects are exemplified by the images shown in Figure 1.

B. Tissue equivalence

Table 2 shows the physical properties of the phantom samples used in this study, identified via analysis of CT data. These results indicate that the cylindrical 3D-printed phantoms all exhibit densities and attenuation coefficients that fall into the range of values identified in the commercial tissue-equivalent materials.

Table 2 Phantom physical properties: Density (ρ), electron density relative to water ($\rho_{e,rel}$) and linear attenuation coefficient relative to water (μ_{rel}).

Phantom	ρ	$\rho_{e,rel}$	μ_{rel}
Cylinder – 90% ABS	1.06 ± 0.02	1.05 ± 0.03	1.04 ± 0.03
Cylinder – 50% ABS	0.58 ± 0.02	0.57 ± 0.02	0.56 ± 0.02
Cylinder – 30% ABS	0.36 ± 0.01	0.35 ± 0.01	0.34 ± 0.01
Lung – 10% ABS	0.17 ± 0.16	0.16 ± 0.16	0.15 ± 0.15
CT-ED Lung-300	0.29 ± 0.02	0.28 ± 0.02	0.26 ± 0.02
CT-ED Lung-450	0.44 ± 0.02	0.44 ± 0.02	0.44 ± 0.02
CT-ED Adipose	0.94 ± 0.01	0.93 ± 0.01	0.90 ± 0.01
CT-ED Liver	1.09 ± 0.01	1.06 ± 0.01	1.07 ± 0.01
CT-ED Cortical bone	1.83 ± 0.02	1.70 ± 0.02	2.23 ± 0.03
CT-ED Solid water	1.02 ± 0.01	1.01 ± 0.01	1.01 ± 0.01
Water	1.00	1.00	1.00

The results for the 90% ABS cylinder lie between the values for the water-equivalent and liver-equivalent inserts from the tissue characterization phantom, potentially providing a useful approximation of tumour, muscle or other soft tissue.

The results for the 30% and 50% ABS cylinders are similar to the values for the two lung-equivalent phantom inserts, making them potentially suitable for use in the construction of lung-equivalent phantoms. The use of a meshed printing technique to produce these low-density samples does appear to have affected their results, because the resulting meshes are very fine and foam-like.

By contrast, the mesh produced by the 3D printing software, when required to produce a phantom with a 10% ABS infill density was so coarse that a structure consisting of solid ABS walls around relatively large (6 mm diameter) air chambers was clearly resolvable in the CT images of the 3D printed lung phantom (see Figure 1). For this reason, the standard deviations in the densities and attenuation coefficients listed for the 10% ABS lung phantom, in table 2, are relatively large and the material fails to approximate the radiological effect of lung tissue.

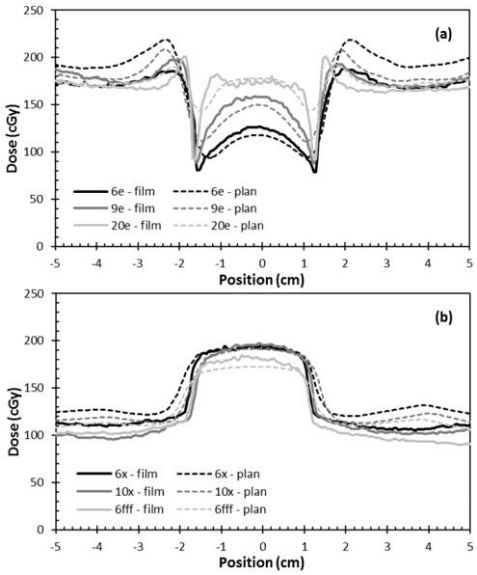

Fig. 2 Dose profiles from (a) electron beams and (b) photon beams, resulting from treatment planning system dose calculations and film measurements, downstream of 30% ABS cylindrical phantom.

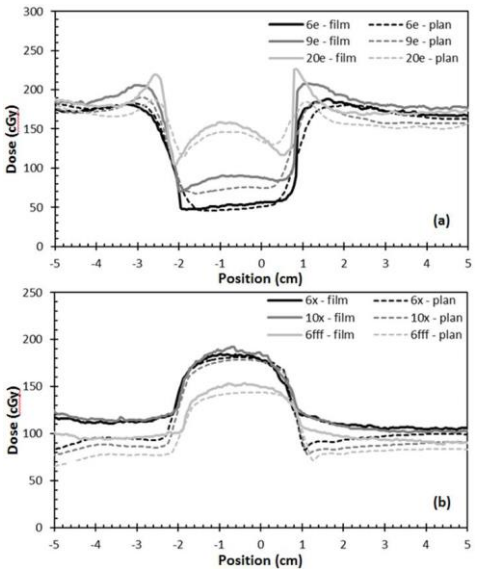

Fig. 3 Dose profiles from (a) electron beams and (b) photon beams, resulting from treatment planning system dose calculations and film measurements, downstream of "LN-300" lung-equivalent insert from Gammex tissue characterization phantom.

Comparisons of film measurements made downstream of the cylindrical 3D printed phantoms and the inserts from the commercial tissue characterization phantom confirm that the attenuation and scattering effects of the 3D printed samples are similar to the effects of established lung- and tissue-equivalent materials, for the eight clinical photon and electron radiotherapy treatment beams used in this study. Planned and measured doses differed by less than 10%, downstream of all 3D printed cylinders and commercial tissue-equivalent samples. Figures 1(a)-(b) and 2(a)-(b) typify these results, for the 30% ABS printed cylinder and the "Lung-300" commercial phantom insert, respectively.

The example dose profiles in Figures 1(a)-(b) and 2(a)-(b) show that directly downstream of both the 3D printed cylinder and the commercial lung-equivalent tissue phantom insert, there is relatively close agreement between the dose predicted by the treatment planning system and dose measured with film, for the two flattened photon beams, while the planned dose slightly exceeds the measured dose, in both cases, for the flattening filter free 6 MV photon beam and the electron beams.

C. Radiation hardness

Data listed in Table 3, indicate that the irradiation of the cylindrical 3D printed phantoms had no noticeable effect on their observed characteristics. The phantoms' densities and dimensions were unchanged (compare with Tables 1 and 2).

Table 3 Measured dimensions and physical properties of sample phantoms, after extensive irradiation.

Phantom	Diameter	Length	ρ	$\rho_{e,rel}$
Cylinder – 90% ABS	3.0	3.9	1.05	1.05
Cylinder – 50% ABS	3.0	3.9	0.58	0.57
Cylinder – 30% ABS	3.0	3.9	0.37	0.37

IV. Conclusions

This study showed that 3D printing using ABS can produce geometrically accurate and radiologically robust materials that are potentially useful as lung- and tissue-equivalent phantoms. A 90% ABS infill density was found to result in a material suitable for modelling tumour, muscle or other soft tissue, while ABS infill densities of 30-50% resulted in phantoms with densities low enough to model lung while also avoiding the course mesh structures that occur when lower infill densities (such as 10% ABS) are used. The data relating ABS infill to electron density produced by this study may be used as calibration information, so that appropriate ABS infill densities can be selected for modelling specific tissues, when printing more complex, anatomical phantoms, in the future.

Conflict of Interest

The authors declare that they have no conflict of interest.

References

1. Lambrecht J T, Berndt D C, Schumacher R, Zehnder M (2009) Generation of three-dimensional prototype models based on cone beam computed tomography. Int. J. comp. Assist. Radiol. Surg. 4(2):175-180
2. Schievano S, Migliavacca F, Coats L, et al. (2007) Percutaneous Pulmonary Valve Implantation Based on Rapid Prototyping of Right Ventricular Outflow Tract and Pulmonary Trunk from MR Data. Radiol. 242(2):490-497
3. Rengier F, Mehndiratta A, von Tengg-Kobligk H, et al. (2010). 3D printing based on imaging data: review of medical applications. Int. J. comp. Assist. Radiol. Surg. 5(4):335-341
4. Bibb R, Winder J (2010). A review of the issues surrounding three-dimensional computed tomography for medical modelling using rapid prototyping techniques. Radiogr. 16(1):78-83
5. Harrison K M, Ebert M A, Kron T, et al. (2011). Design, manufacture, and evaluation of an anthropomorphic pelvic phantom purpose-built for radiotherapy dosimetric intercomparison. Med. Phys. 38(10):5330-5337
6. Kim J I, Choi H, Lee B I, et al. (2006). Physical phantom of typical Korean male for radiation protection purpose. Radiat. Prot. Dosim. 118(1):131-136
7. Nizam A, Gopal R N, Naing L, et al. (2006). Dimensional accuracy of the skull models produced by rapid prototyping technology using stereolithography apparatus. Orofac. Sci. 1:60-66
8. Su S, Moran K, Robar J L. (2013). Design and production of 3D printed bolus for electron radiation therapy. J. Appl. clin. Med. Phys. 15(4):4831-4831
9. Followill D S, Evans D R, Cherry C, et al. (2007). Design, development, and implementation of the radiological physics center's pelvis and thorax anthropomorphic quality assurance phantoms. Med. Phys. 34(6):2070-2076
10. Deasy J O, Blanco A I, Clark V H. (2003) CERR: a computational environment for radiotherapy research. Med. Phys. 30:979–985
11. Fedorov A, Beichel R, Kalpathy-Cramer J, et al. (2012) 3D Slicer as an Image Computing Platform for the Quantitative Imaging Network. Magn. Reson. Imaging. 30(9):1323-1341
12. Kairn T, Aland T, Kenny J. (2010) Local heterogeneities in early batches of EBT2 film: A suggested solution. Phys. Med. Biol. 55(15):L37-L42
13. Aland T, Kairn T, Kenny J. (2011) Evaluation of a Gafchromic EBT2 film dosimetry system for radiotherapy quality assurance. Australas. Phys. Eng. Sci. Med. 34(2):251-260

Author: T. Kairn
Institute: Genesis CancerCare Queensland
Street: Suite 1, 40 Chasely St
City: Auchenflower 4066
Country: Australia
Email: t.kairn@gmail.com